INORGANIC CHEMISTRY
FRONTIERS

REVIEW

View Article Online
View Journal | View Issue

Cite this: *Inorg. Chem. Front.*, 2019, **6**, 1623

Diazido platinum(IV) complexes for photoactivated anticancer chemotherapy

Huayun Shi, Cinzia Imberti and Peter J. Sadler *

Diazido Pt(IV) complexes with a general formula $[Pt(N_3)_2(L)(L')(OR)(OR')]$ are a new generation of anticancer prodrugs designed for use in photoactivated chemotherapy. The potencies of these complexes are affected by the *cis*/*trans* geometry configuration, the non-leaving ligand L/L' and derivatisation of the axial ligand OR/OR'. Diazido Pt(IV) complexes exhibit high dark stability and promising photocytotoxicity circumventing cisplatin resistance. Upon irradiation, diazido Pt(IV) complexes release anticancer active Pt(II) species, azidyl radicals and ROS, which interact with biomolecules and therefore affect the cellular components and pathways. The conjugation of diazido Pt(IV) complexes with anticancer drugs or cancer-targeting vectors is an effective strategy to optimise the design of these photoactive prodrugs. Diazido Pt(IV) complexes represent a series of promising anticancer prodrugs owing to their novel mechanism of action which differs from that of classical cisplatin and its analogues.

Received 15th March 2019,
Accepted 26th April 2019

DOI: 10.1039/c9qi00288j

rsc.li/frontiers-inorganic

1. Introduction

The treatment of cancer, a group of diseases involving uncontrolled growth and spread of cells and representing the leading cause of death globally, remains a major challenge.[1] Phototherapy, consisting of photodynamic therapy (PDT) and photoactivated chemotherapy (PACT), has attracted much attention in cancer treatment due to its high spatial-temporal controllability and minimal invasiveness. The mechanism of action of clinically approved PDT is based on the combination of a photosensitiser, light and oxygen.[2] High oxygen dependence limits the application of PDT since the oxygen concentration in hypoxic tumours is low. PACT, in contrast to PDT, is an oxygen-independent phototherapy, which involves chemical changes of prodrugs upon irradiation and provides a new avenue in anticancer drug development.[3,4]

The serendipitous discovery of the antiproliferative properties of cisplatin in 1968 by Rosenberg *et al.* stimulated a

Department of Chemistry, University of Warwick, Coventry, CV4 7AL, UK.
E-mail: p.j.sadler@warwick.ac.uk

Huayun Shi

Huayun Shi obtained her BSc degree in Chemistry from Sun Yat-sen University in Guangzhou (China), and was awarded a University of Warwick (UK) Chancellor's International Scholarship in 2015 to study for her PhD in Peter Sadler's group. Her research is focused on the design of novel photoactive platinum complexes with azide ligands for cancer therapy, and elucidation of their mechanism of action.

Cinzia Imberti

Cinzia Imberti obtained a M.Sci degree in Chemistry at the University of Padova (Italy) in 2012. She then obtained a PhD at King's College London, working on the development of new radiometal-based radiopharmaceuticals under the supervision of Professor Philip J. Blower. On completion of her PhD she was awarded a Sir Henry Wellcome Postdoctoral Fellowship and joined Peter Sadler's group at the University of Warwick in 2018. Her research is focussed on the mechanism of action of platinum-based anticancer agents with particular emphasis on photoactivatable platinum complexes.

Table 1 Comparative properties of bioactive platinum complexes[11–15]

Pt complexes	Mechanism of action	Advantages	Disadvantages	Ref.
Cisplatin-like Pt(II) complexes	Hydrolysis, covalent DNA binding	FDA approved, high cure rate	Poor pharmacokinetics, dose-limiting side effects, restricted anticancer spectrum, lack of selectivity, high incidence of resistance	5 and 6
Pt(II) complexes different from cisplatin	Covalent or non-covalent DNA binding	Overcome cisplatin resistance	Limited selectivity, inherent systemic toxicity	16–19
Photosensitive Pt(II) complexes	Excitation of triplet oxygen (PDT)	Good photoselectivity, overcome cisplatin resistance	Oxygen dependence, limited λ_{ex} wavelength range	20 and 21
Photoactive Pt(II) complexes	Photoactivation to form cytotoxic Pt(II) species (PACT)	Oxygen independence	High dark cytotoxicity, low photocytotoxic indices	45–53
Chemically reductive Pt(IV) complexes	Reduction by bio-reductants	Easy modification, improved selectivity and cellular accumulation	Poor stability before entering cells	30–32
Photoactive Pt(IV) complexes	Photoreduction to release cytotoxic Pt(II) species and radicals (PACT)	Oxygen independence, good dark stability, overcome cisplatin resistance, spatial and temporal selectivity, easy modification	Low photocytotoxic indices, short λ_{ex} wavelength range, limited light penetration	62, 68, 77 and 81

wide research for other platinum-based anticancer drugs.[5,6] Platinum drugs are now used to treat over 40% of all cancer patients in chemotherapy since cisplatin was approved by FDA in 1978 to treat testicular and ovarian cancers.[7–10] Several classes of platinum anticancer agents, as summarised in Table 1, have been investigated in the past decades and extensively reviewed in recent publications.[11–21] Compared with Pt(II) complexes,[22] Pt(IV) complexes with d^6 electronic configuration are more kinetically inert to ligand substitution, and more stable under physiological conditions.[14,23] Pt(IV) complexes can be reduced by bio-reductants (*e.g.* GSH, ascorbic acid, cysteine) to form active Pt(II) species through which they exert their anticancer activity.[24–26] Although some Pt(IV) complexes entered clinical trials, none of them has been approved for clinical use.[27–32]

Peter J Sadler

Peter Sadler obtained his BA, MA and DPhil at the University of Oxford. Subsequently he was a MRC Research Fellow at the University of Cambridge and National Institute for Medical Research. From 1973–96 he was Lecturer, Reader and Professor at Birkbeck College, University of London, and from 1996–2007 Crum Brown Chair of Chemistry at the University of Edinburgh. Then he became Head of the Department of Chemistry at the University of Warwick, where he is now a Professor. He is a Fellow of the Royal Society of Chemistry (FRSC), Royal Society of Edinburgh (FRSE) and the Royal Society of London (FRS), and an EPSRC RISE Fellow (Recognising Inspirational Scientists and Engineers).

Notably, photodecomposition is a prominent feature of Pt(IV) complexes, suggesting their potential as PACT prodrugs.[15,33–35] Transition metal azido complexes are usually light sensitive.[36,37] The first photoreductive Pt(IV) complex with azide ligands reported by Vogler *et al.* in 1978 was *trans*-$[Pt(N_3)_2(CN)_4]^{2-}$.[38] Upon irradiation with UVA at 302 nm, the wavelength of its maximum electronic absorbance, assigned as a ligand-to-metal ($N_3 \rightarrow Pt$) charge-transfer transition, *trans*-$[Pt(N_3)_2(CN)_4]^{2-}$ was converted to $[Pt(CN)_4]^{2-}$ *via* the formation of two azidyl radicals without a Pt(III) intermediate. The unstable azidyl radicals released nitrogen gas, preventing the re-oxidation of the platinum centre.[36] Another azido Pt(IV) complex $[Pt(N_3)_6]^{2-}$ was found to undergo photoreduction, yielding $[Pt(N_3)_4]^{2-}$ and even metallic Pt, accompanied by the release of nitrogen gas.[39,40] These early studies provided a basis for our group to develop diazido Pt(IV) complexes that are stable in the dark, and exhibit promising cytotoxicity upon irradiation.[11,15,34,35,41,42]

In this review, our discussion begins with a brief introduction to photoactivated chemotherapy and focuses on the development of photoactive diazido Pt(IV) complexes, including the design of new complexes, their photochemistry and photobiology, mechanism of action, derivatisation of axial ligands and conjugation to nanoparticles to improve photocytotoxicity and selectivity. We give a comprehensive description of diazido Pt(IV) complexes and consider feasible strategies for their future clinical use.

2. Photoactivated chemotherapy

PACT relies on light-mediated chemical changes, transforming an inactive prodrug into an active agent upon irradiation.[3,4,43,44] Platinum-based PACT anticancer drugs can be activated *via* different mechanisms as described below.

• *Photoreduction*: Pt(IV) complexes can be reduced upon irradiation to release cytotoxic Pt(II) species and ligands.[34,41]

• *Photosubstitution*: Pt(II) complexes with photolabile ligand (*e.g.* curcumin) undergo ligand dissociation followed by solvent substitution.[45–49]

• *Photocleavage of ligand*: Photon absorption by the metal centre can result in the cleavage of organic bonds, (*e.g.* C–N, N–O) in photosensitive *o*-nitrobenzyl alcohol derivatives coordinated to platinum.[50,51]

• *Photoswitching*: Pt(II) complexes bridged by a diarylethene ligand change the configuration of the ligand upon irradiation to alter the cytotoxic properties.[52,53]

Although PACT is often compared with PDT since they both require light to activate relatively non-toxic drugs, these two classes of treatments present many differences.[4] Generally, PACT agents decompose upon irradiation, while PDT agents are photostable. Notably, the oxygen-independent mechanism of action of PACT agents improves their efficiency in hypoxic tumours and represents a major advantage of PACT over PDT.

However, the development of PACT is still in its infancy, and the current performance of PACT complexes is not competitive with PDT photosensitisers.[4] Some photosensitisers in clinical trials exhibit extremely high photocytotoxicity indices (photo-cytotoxicity/dark-cytotoxicity, *e.g.* **TLD-1433**, up to 10^5),[54] and some can be excited by near infrared (NIR) irradiation (*e.g.* **WST-09**, 763 nm).[55] In contrast, the highest reported photocytotoxicity index of PACT agents is 1880,[56] and the longest excitation wavelengths reported for simple metal complex-based PACT agents are in the red region, which limits light penetration into tissue to a depth of *ca.* 5 mm.[57–59] To enter clinical trials, more effort needs to be invested into the preclinical development of new PACT complexes.

3. Development of photoactive Pt(IV) complexes

In general, photoactive Pt(IV) complexes contain axial, non-leaving, and leaving ligands. Axial ligands can be used to tune the physical and chemical properties of the complexes without altering the structure of the active pharmacophore that is ultimately released.[60] Non-leaving ligands do not significantly alter the reduction potential of Pt(IV) complexes and can be varied to change their properties without reducing the dark stability.[61] Leaving ligands play key roles in photoactive Pt(IV) complexes. Two main classes of Pt(IV) complexes, namely diiodo- and diazido-Pt(IV) complexes, have been investigated as photoactive Pt(IV) anticancer prodrugs (Scheme 1).

Diiodo-Pt(IV)-ethylenediamines bearing various axial ligands (Cl, OH, $OCOCH_3$, OSO_2CH_3, or $OCOCF_3$) were reported by Kratochwil *et al.* in 1996 as the first-generation photoactive Pt(IV) complexes with a general formula *trans*, *cis*-$[Pt(X)_2I_2(en)]$ (Fig. 1).[62–66] Iodide is a weak field ligand with a low optical electronegativity,[67] and thus the LMCT bands of these complexes are centred at the relatively longer wavelength of *ca.* 400 nm with a tail extending out into the visible range.[62] As a result, all of these complexes are photolabile to light λ_{irr} > 375 nm. However, their application is limited due to their poor dark stability, which might be due to facile cellular bioreduction. For example, electron donation to Pt(IV) can occur through thiolate attack on iodide ligands.[65]

The second-generation photoactive Pt(IV) complexes with azide ligands, were developed later to achieve better dark stability and photobiological properties with a general formula $[Pt(N_3)_2(L)(L')(OR)(OR')]$ (Fig. 2, Table 2). The first diazido-Pt(IV) complexes, *cis*, *trans*-$[Pt(en)(N_3)_2(OH)_2]$ (**1**) and *cis*, *trans*, *cis*-$[Pt(N_3)_2(OH)_2(NH_3)_2]$ (**2**) were reported in 2003.[68] Cytotoxicity studies showed that these complexes caused very low inhibition of growth in the dark, but significantly enhanced cytotoxicity upon irradiation in both 5637 bladder

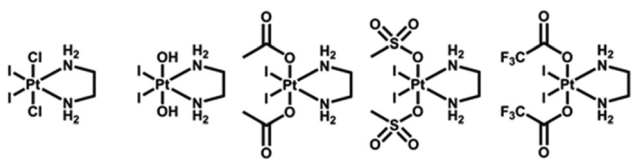

Fig. 1 First-generation photoactive diiodo-Pt(IV) complexes.

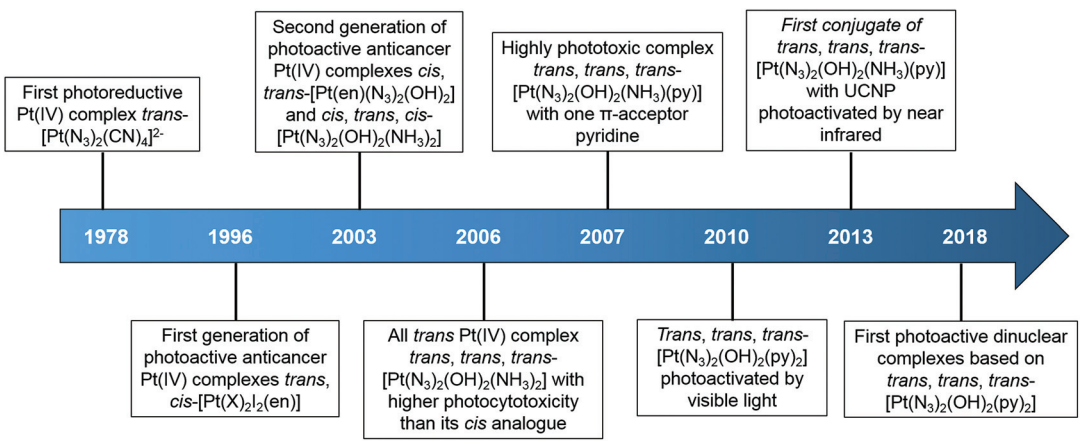

Scheme 1 Timeline illustrating the publication year for important photoactive Pt(IV) complexes.

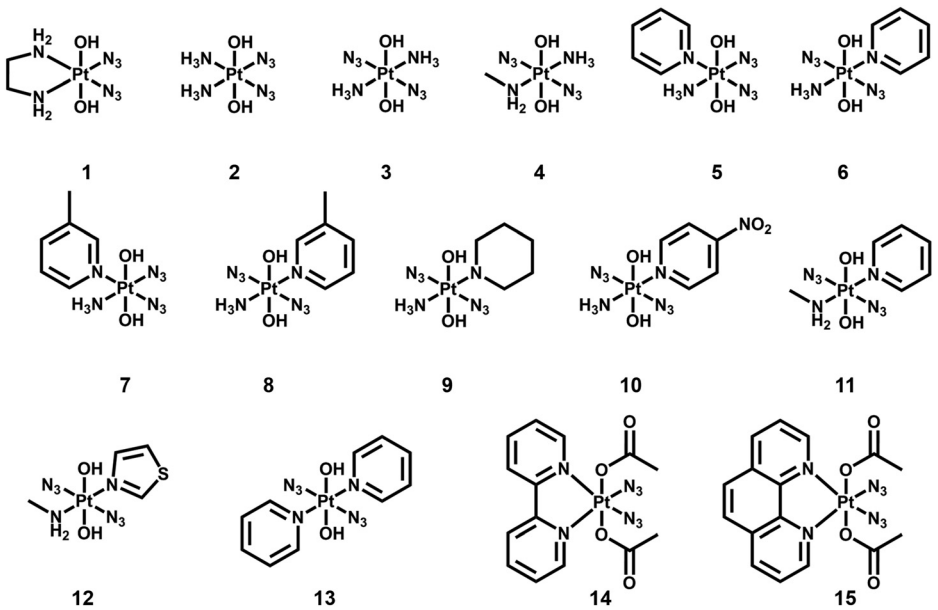

Fig. 2 Selected second-generation photoactive diazido-platinum(IV) complexes.

Table 2 LMCT bands and IC_{50} values for selected photoactive diazido-Pt(IV) complexes

Complex	Non-leaving ligands			LMCT band λ_{max} nm^{-1} ($N_3 \rightarrow Pt$)	λ_{irr}/nm	Cell line	IC_{50} values[a]/μM			Ref.
	L_1	L_2	*cis*/*trans*				Light	Dark	PI	
$[Pt(N_3)_2(CN)_4]^{2-}$	CN	CN	*t*	302	302	—	—	—	—	38
$[Pt(N_3)_6]^{2-}$	—		—	308	314	—	—	—	—	39 and 40
1	en		*c*	315	365	5637	63.0 ± 20.2	440 ± 143	7.0	68 and 69
					365	5637-CDDP	79.8 ± 16.6	>200	>2.5	
2	NH_3	NH_3	*c*	256	365	5637	49.3 ± 28.1	357 ± 81	7.2	68 and 69
					365	HaCaT	169.3	>287.9	>1.7	74
3	NH_3	NH_3	*t*	285	365	HaCaT	121.2	>287.9	>2.4	70 and 74
4	NH_3	MA	*t*	286	365	HaCaT	65.6	>276.8	>4.2	74 and 76
5	NH_3	Py	*c*	258	365	HaCaT	100.9	>244.4	>2.4	74
6	NH_3	Py	*t*	289	365	HaCaT	6.8	>244.4	>35.9	74 and 77
7	NH_3		*c*	259	365	HaCaT	>236.2	>236.2	—	74
8	NH_3		*t*	289	365	HaCaT	22.0	144.1	6.6	74 and 76
9	NH_3		*t*	288	366	5637	29.17 ± 2.23	>80	>2.7	79
10	NH_3	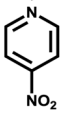	*t*	287	365	—	—	—	—	75
11	Py	MA	*t*	289	365	HaCaT	2.6	>236.3	>90.8	80
					420	HaCaT	14.7	>236.3	>16.0	
12	Tz	MA	*t*	289	365	HaCaT	3.5	>232.9	>66.5	80
					420	HaCaT	11.2	>232.9	>20.7	
13	Py	Py	*t*	294	365	HaCaT	1.4	>212.3	>151.6	81
					420	HaCaT	9.5	>212.3	>22.3	
					365	A2780	1.4	>212.3	>151.6	
					365	A2780cis	14.5	>212.3	>14.6	
14	Bpy		*c*	304/315	365	—	—	—	—	83
15	Phen		*c*	300	365	—	—	—	—	83

[a] Note that IC_{50} values were obtained *via* different methods/conditions. PI = Photocytotoxicity index.

cells and cisplatin-resistant 5637 bladder cells, even though to a less extent than cisplatin.[69]

Intriguingly, the all *trans* photoactive Pt(IV) prodrug, *trans*, *trans*, *trans*-$[Pt(N_3)_2(OH)_2(NH_3)_2]$ (**3**), exhibited higher aqueous solubility and a more intense and red-shifted LMCT band compared with its *cis* isomer **2**.[70] Higher photocytotoxicity induced by **3** upon irradiation (as toxic as cisplatin) was determined in cancer cells, which was in contrast to the early structure–activity relationship for classical anticancer platinum complexes that the *cis* geometry was more favourable.[71–73] Comparisons between other diazido Pt(IV) complexes incorporating a wide range of aliphatic and aromatic amines confirmed the higher potency of the *trans* configuration.[74,75]

The introduction of a methyl substituent into an ammonia ligand improved the photocytotoxicity of the Pt(IV) complexes *trans*, *trans*, *trans*-$[Pt(N_3)_2(OH)_2(NH_3)(MA)]$ (**4**, MA = methylamine).[74,76] Furthermore, replacement of an ammine ligand in **3** by a π-acceptor pyridine (Py) ligand resulted in the highly phototoxic complex *trans*, *trans*, *trans*-$[Pt(N_3)_2(OH)_2(NH_3)(Py)]$ (**6**) that showed 13–80× higher photocytotoxicity compared with cisplatin, and 15× higher towards cisplatin-resistant human ovarian A2780cis cells.[77] Notably, **6** is the only simple diazido-Pt(IV) prodrug that has been tested *in vivo*. Two of seven nude mice bearing OE19 oesophageal cancer xenografts treated with **6** at low dose with short irradiation times (420 nm, 100 J cm^{-2}, 2 × 30 min) survived at 35 days, while none of the control mice without drug or irradiation survived, and the complex was well tolerated.[78] Encouraged by the success of **6**, a series of ligands was introduced to replace one or both of the ammine ligands. The replacement of pyridine by 3-methylpyridine (**8**),[74,76] piperidine (**9**),[79] or 4-nitro-pyridine (**10**)[75] did not result in significant differences. Higher cytotoxicity of complexes with methylamine *trans*, *trans*, *trans*-$[Pt(N_3)_2(OH)_2(MA)(Py)]$ (**11**) and *trans*, *trans*, *trans*-$[Pt(N_3)_2(OH)_2(MA)(Tz)]$ (**12**, Tz = thiazole) was attributed to the high stability of Pt–MA bonds.[80] In addition, the Tz-containing analogue **12** was more effective towards the cisplatin resistant cell lines.

The key role of pyridine ligands in the high phototoxicity and the mechanism of action different from cisplatin promoted the development of a novel diazido-Pt(IV) complex with two pyridine ligands, *trans*, *trans*, *trans*-$[Pt(N_3)_2(OH)_2(Py)_2]$ (**13**).[81] Upon irradiation with UVA or visible blue light, **13** exhibited significant toxicity toward a number of human cell lines with high phototoxicity indices. Dinuclear complexes based on **13** also displayed photodecomposition with blue light irradiation.[82]

Diazido-Pt(IV) complexes incorporating π-conjugated bidentate diimine ligands *trans*, *cis*-$[Pt(2,2'\text{-Bpy})(OAc)_2(N_3)_2]$ (**14**, 2,2′-Bpy = 2,2′-bipyridine) and *trans*, *cis*-$[Pt(Phen)(OAc)_2(N_3)_2]$ (**15**, Phen = phenanthroline) exhibited greater absorption at longer wavelengths compared with previously reported diazido-Pt(IV) complexes.[83] Their photodecompositions were observed upon irradiation with both UVA and visible green light.

Other than iodide and azide, chloride is also a potential candidate as leaving ligand for photoactive Pt(IV) complexes.

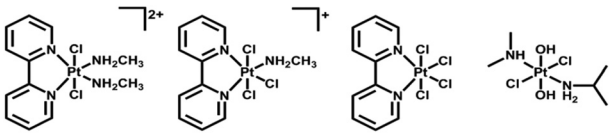

Fig. 3 Photoactive Pt(IV) complexes with chlorides as leaving ligands.

Upon irradiation, photoreduction to Pt(II) species was observed for *trans*-$[PtCl_2(2,2'\text{-Bpy})(MA)_2]Cl_2$, *mer*-$[PtCl_3(2,2'\text{-Bpy})(MA)]Cl$, $[PtCl_4(2,2'\text{-Bpy})]$, and *trans*, *trans*, *trans*-$[PtCl_2(OH)_2(DMA)(IPA)]$ (Fig. 3, DMA = dimethylamine, IPA = isopropylamine).[84–86] Some Pt(IV) complexes with chloride ligands, such as oxoplatin, even though not photoactive on their own, exhibit photorelease of Pt(II) species when conjugated to specific nanoparticles.[87,88]

4. Photochemistry and photobiology of diazido Pt(IV) complexes

4.1. Photodecomposition pathways

Photodecomposition of diazido Pt(IV) complexes mainly relies on the reduction of Pt(IV) and the release of azide ligands triggered by light (Fig. 4a).[38] The strong absorbance, assigned to a dissociative LMCT band ($N_3 \rightarrow Pt$), is a key transition in photodecomposition.[70,74,75] Upon irradiation, a rapid decrease in intensity of the LMCT band can be observed for diazido Pt(IV) complexes due to the release of azide ligands (Fig. 4b and c).[38,41] The wavelength of the LMCT band is affected significantly by the overall configuration of Pt(IV).[70,74,75,89] In general, complexes with *cis*-$\{Pt^{IV}(N_3)_2\}$ motifs exhibit LMCT bands at shorter wavelength (*ca.* 260 nm), while those of *trans* isomers are red-shifted by 30 nm (*ca.* 290 nm) (Table 2).[74] However, complexes with bidentate chelating non-leaving ligands display LMCT bands at longer wavelength (*ca.* 300 nm) than diazido Pt(IV) complexes with only monodentate ligands, despite of their *cis* configuration.[68,83,89] Electronic transitions

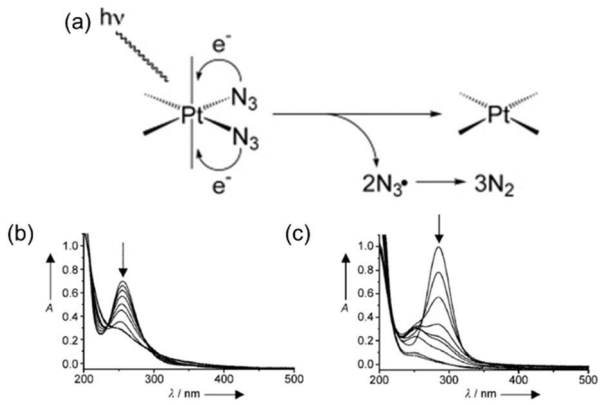

Fig. 4 (a) A possible mechanism for the photoreduction of diazido-Pt(IV) complexes;[91] UV-vis spectral changes for (b) **2** and (c) **3** in aqueous solution upon UVA irradiation.[70] Adapted from ref. 91 and 70.

for *cis* isomers tend to arise from transitions from orbitals of the azide ligands to metal d orbitals, whereas those for all-*trans* isomers are more likely to arise from both axial and azide ligands to the metal d orbitals, and thus lead to different photoproducts.[75] The electron-donating and steric properties of non-leaving ligands are also important factors which affect the LMCT band. The replacement of NH_3 by a π-acceptor pyridine ligand results in a red-shift of the intense LMCT band (*ca.* 5 nm for each substitution).[70,77,81] The substituents on pyridine ligands affect the maximum absorption slightly.[75]

The low-intensity transitions (the "tail") that have mixed dissociative ^{1}LMCT/^{1}IL (IL = interligand) character might account for the photoactivity induced by longer wavelength activation,[75,81] which is a major challenge in the development of new diazido Pt(IV) complexes. The low-intensity transitions have significant contributions from the LUMO orbital that is strongly σ-antibonding towards the two Pt–N_3 bonds.[81] Light excitation to populate this orbital induces elongation of the Pt–N_3 bond, and eventually leads to azide release.[81] The weak absorption of **13** in the blue region (414 nm) might be responsible for its photodecomposition with visible light.[81]

Much effort has been devoted to the investigation of the photodecomposition pathways of the most promising diazido Pt(IV) complexes. The early studies suggested that the photodecomposition involved the release of two azide ligands as $N_3^{\bullet}$ radicals, which can combine to form N_2 molecules.[38] However, during further investigation of diazido Pt(IV) complexes, different pathways have been proposed depending on the configuration of Pt(IV), non-leaving ligands, and the solution environment.

1D ^{14}N{^{1}H} NMR spectra of ^{15}N-labelled **2** with two $^{15}NH_3$ in acidic aqueous solution (pH = 5.1) upon irradiation with UVA (365 nm) suggested the formation of N_2 and unlabelled free NH_3, with a pH increased to 10.7 and O_2 liberation detected.[90] In addition, the major Pt(II) species detected was assigned to *trans*-$[Pt(NH_3)_2(H_2O)_2]^{2+}$, indicating photoisomerisation with photoreduction. Nitrene intermediates generated during the photodecomposition were trapped by dimethyl sulphide (DMS), which suggested a possible new mechanism.[90] However, the photodecomposition of **2** in PBS involved the photosubstitution of at least one azide ligand by H_2O/OH and the release of azide ions (Fig. 5).[91] Ammonia ligands were also released from Pt(IV) as confirmed by NMR with an increase in pH. After replacement of both azides (or even ammonia ligands) by H_2O/OH, photoreduction may occur by one-electron transfers from each of two hydroxide groups coordinated to the Pt(IV) leading to some species containing *trans*-{$Pt(OH)_2$} motifs and hydroxyl radicals. DFT and TD-DFT calculations demonstrated the theoretical possibility of the replacement of both NH_3 and N_3 groups *trans* to each other by H_2O/OH.[92]

The photodecomposition pathways for **3** in PBS and acidic solution are similar to that of its *cis* isomer **2**, in which the azide ion was detected in PBS, while N_2 was found in acidic solution.[93] *Trans* Pt(II) species, O_2 and free ammonia were detected as photoproducts of **3** with a subsequent increase in pH in both basic and acidic solution. However, the *trans* isomer **3** gave fewer types of Pt species in acidic solution, but more minor side-products and less hydroxo-/oxo-bridged species compared to its *cis* isomer **2**.[93] In addition, no photoisomerisation was observed in the photodecomposition of **3**.

Even though azidyl radicals are regarded as important cytotoxic photoproducts of diazido Pt(IV) complexes, they were not considered further in the early work.[90–93] A recent study on the first stage of photodecomposition using ultrafast kinetic spectroscopy and nanosecond laser flash photolysis suggested that the photodecomposition of both *cis* **2** and *trans* **3** is a chain process beginning with the replacement of one azide ligand by a water molecule and the release of azidyl radicals.[94] Two successive Pt(III) intermediates participated in chain initiation and $[Pt^{III}(NH_3)_2(OH)_2]^+$ was a chain carrier.

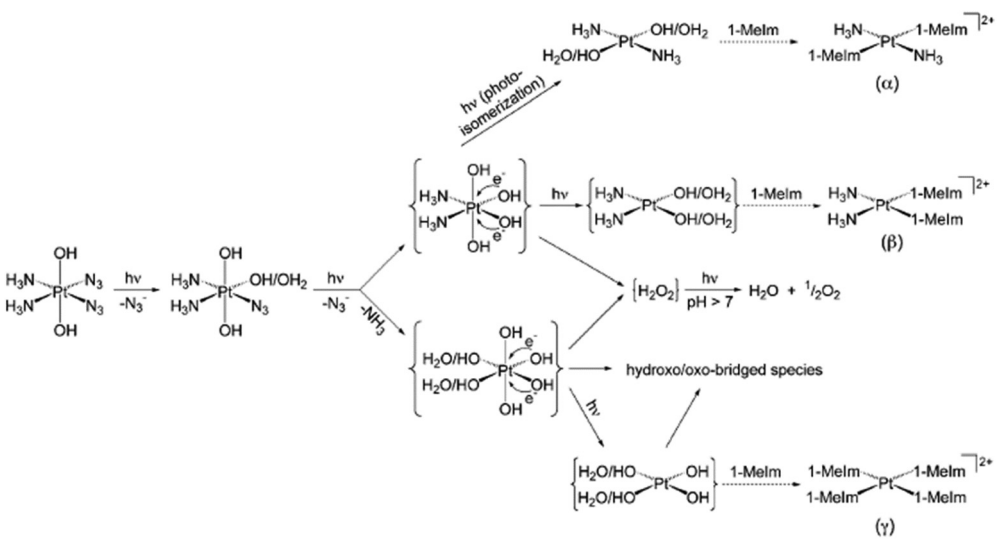

Fig. 5 Possible pathways for photodecomposition and photoreactions of complex **2** with 1-methylimidazole in PBS. Adapted from ref. 91.

Trans-$[Pt(OH)_4(^{15}NH_3)(Py)]$ and *trans*-$[Pt(N_3)(OH)_3(^{15}NH_3)(Py)]$ were detected as photoproducts of **6** using $^{15}NH_3$ and 1D ^1H and 2D [^1H, ^{15}N] HSQC NMR spectroscopy, indicating the release of azides.[77] In contrast, no evidence of pyridine release was found. Furthermore, very little reduction to Pt(II) species was detected by NMR. Consistently, $[Pt(OH)_2NH_3(Py)]$ and $[Pt(OH)(N_3)(NH_3)(Py)]$ at low concentration were detected by LC-MS.[95] In addition, $[Pt(N_3)_3(OH)(NH_3)(Py)]$ was observed by LC-MS as a photosubstitution product of **6** as well as azide ions, indicating the release of azide ligands.[95] No platinum species without pyridine were detected by LC-MS, in accordance with NMR data. However, no detailed photodecomposition pathway has been proposed for **6** so far. For its piperidine analogue **9**, only $[Pt(OH)_2(piperidine)NH_3]$ was detected as a product by LC-MS, suggesting an effect of the heterocyclic ring on the photodecomposition pathways.[96] The MA analogue of **6**, **11** produced N_2, N_3^-, N_3 radicals and $^1O_2$ upon irradiation, with Pt–nitrene intermediates involved in the pathway (Fig. 6).[97]

Comprehensive spectroscopic studies of the photodecomposition of the most promising diazido Pt(IV) complex **13** have been performed by Attenuated Total Reflection Fourier Transform Infrared (ATR-FTIR) and NMR.[81,98] ATR-FTIR revealed the binding of water to platinum in the final product, which was assigned as *trans*-$[Pt^{II}(Py)_2(H_2O/OH)_2]$ fitted by Multi-Curve Resolution Alternating Least Squares (MCR-ALS). *Trans*-$[Pt^{II}(N_3)(Py)_2(H_2O/OH)]$ was detected as an intermediate, implying release of at least one hydroxyl radical and one azidyl radical or two hydroxyl radicals during the photoreduction.[98] No pyridine release was detected by ^1H NMR, in contrast to NH_3 complexes, and might contribute to its higher potency.[81]

4.2. Photoreactions with important biomolecules

The cytotoxicity of diazido Pt(IV) complexes is mediated by the photoreduction products, including Pt(II) species, azidyl radicals and ROS, and their interactions with biomolecules, including nucleotides, DNA, amino acids, peptides and proteins.[35,41]

The RNA monomer nucleotide guanosine monophosphate (5′-GMP) is often used as a model for nucleobase guanine, considered to be the major target of Pt anticancer drugs on DNA.[99,100] Unlike Pt(II) complexes, diazido Pt(IV) complexes do not interact with 5′-GMP in the dark, but only upon irradiation, forming mono- and/or bis-GMP adducts. A bis-GMP adduct $[Pt(en)(GMP\text{-}N7)_2]^{2+}$ was detected by NMR when **1** reacted with two mol. equiv. of 5′-GMP upon irradiation with visible light (457.9 nm), while $[Pt(en)\{d(GpG)\text{-}N7^1,N7^2\}]^{2+}$ was the only major photoproduct of **1** in the presence of one mol. equiv. of d(GpG).[68] Similar results were found for **2** and **3**.[68,70] Interestingly, *trans* **3** was able to form a bis(5′-GMP) adduct under UVA irradiation at a faster rate than transplatin.[70] In addition, the photodecomposition of **3** was accelerated in the presence of 5′-GMP, and a few Pt-GMP adducts were even detected upon red light irradiation.[70] For **6**, the Pt(II) mono-GMP adduct $[Pt(N_3)(NH_3)(5'\text{-}GMP)(Py)]^+$ was detected as the initial main photoproduct from reaction with 5′-GMP, while the bis-5′-GMP adduct *trans*-$[Pt(NH_3)(Py)(5'\text{-}GMP)_2]^{2+}$ became predominant at longer irradiation times.[77] Unexpectedly, guanine photooxidation by **11** was observed *via* a mechanism involving $^1O_2$, while the NH_3 ligand in the adducts probably arose from the formation of a Pt–nitrene intermediate (Fig. 6).[97] Both mono- and bis-GMP adducts (*trans*-$[Pt(N_3)(Py)_2(5'\text{-}GMP)]^+$ and *trans*-$[Pt(Py)_2(5'\text{-}GMP)_2]^{2+}$) were detected as photoproducts of **13** and 5′-GMP by NMR, LC-MS and ATR-FTIR spectra.[81,98]

DNA platination photoinduced by **1** with r_b = 0.01 (r_b = Pt coordinated per nucleotide residue) gave a preference for GG sequences, forming bifunctional GG adducts, which is similar to cisplatin.[101] Intriguingly, photoactivated **1** and **2** formed GG adducts more rapidly than cisplatin.[69] Transcription mapping revealed similar major stop sites in a DNA fragment treated with **6** and irradiation or with transplatin, while the level of DNA adducts formed by irradiated **6** was significantly higher than that by cisplatin and transplatin.[77] DNA interstrand cross-links and DNA–protein cross-links were also induced by **6** with light. Remarkably, a plasmid treated with **6** and UVA exhibited considerably lower levels of damage-induced DNA

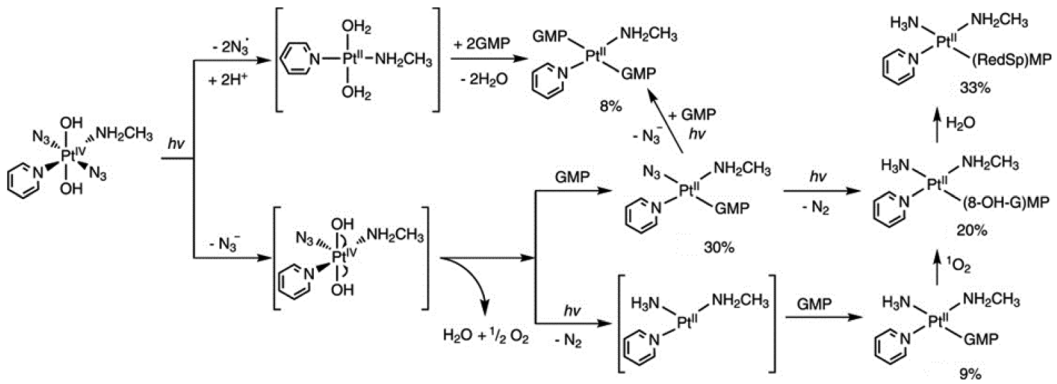

Fig. 6 Possible pathways for photodecomposition and photoreactions of **11** with 5′-GMP upon irradiation with UVA. Adapted from ref. 97.

repair synthesis than those with cisplatin. Significantly larger unwinding angles and a higher percentage of interstrand cross-links were observed when DNA was treated with **11** or **12** compared to cisplatin.[80] The nature of DNA lesions induced by **13** upon irradiation was expected to be different from those induced by cisplatin.[81] Irreversible DNA coordination was observed for **13** with light, including *ca.* 12% interstrand (intramolecular) cross-links, *ca.* 37% monofunctional adducts, and *ca.* 51% intrastrand cross-links.[102] The interstrand cross-links formed by **13** and light were characterised, and the structure of a *trans*-$\{Pt(Py)_2\}^{2+}$-DNA showing a bend toward the minor groove, a global bend of *ca.* 67° and an unwinding of *ca.* 20° was simulated by computational studies (Fig. 7).[103]

Other than nucleotides and DNA, amino acid, peptides and proteins are also targets for Pt(II) species released from diazido Pt(IV) complexes. The photoactivated platinum centre of **2** can also react with dimethyl sulphide, a thioether related to that in the side chain of the amino acid methionine (Met), in acidic solution. The nitrene intermediate formed dimethylsulfilimine adducts that can undergo a Stevens-like rearrangement in which the Pt–N=SMe_2 group becomes Pt–N(H)–CH_2–SMe, giving a *N*-(methylthiomethylene)amido derivative.[90] The derivative can release two hydroxyl radicals upon irradiation.[90] The photoreaction between **2** and 1-methylimidazole, a histidine (His) side chain analogue, in PBS (Fig. 5) gave 6 different Pt-coordinated 1-methylimidazole species, suggesting it can bind to proteins.[91]

Azidyl radicals are potentially key species, which might kill cancer cells by oxidative attack. Azidyl radicals generated by **13** can be trapped by 5,5-dimethyl-1-pyrroline *N*-oxide (DMPO) and detected using EPR (Fig. 8a).[104] However, in the presence of Trp, the azidyl radicals were quenched, which reduced the photocytotoxicity of **13**.[104] The resulting tryptophan (Trp) radicals have been trapped by 2-methyl-2-nitrosopropane (MNP)

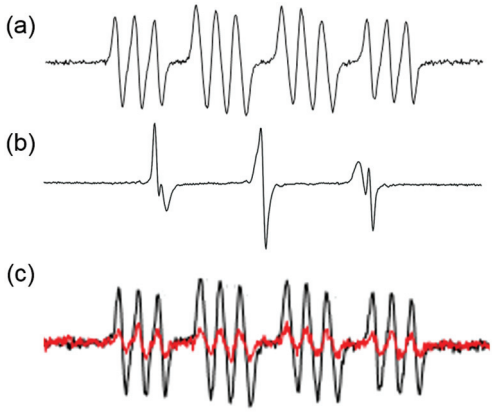

Fig. 8 EPR spectra of **13** in PBS upon irradiation in the presence of spin-traps (a) DMPO for $N_3^{\bullet}$ radicals; (b) Trp + MNP for Trp$^{\bullet}$ radicals (and background DTBN$^{\bullet}$ radicals); (c) pentagastrin + DMPO for $N_3^{\bullet}$ radicals (red: with pentagastrin; black: without pentagastrin). Adapted from ref. 105.

and such radicals might be involved in the cytotoxicity towards cancer cells (Fig. 8b).[105] Background signals from di-*tert*-butyl nitroxide (DTBN) radicals arose from MNP upon irradiation. The Trp containing peptide pentagastrin also quenched azidyl radicals (Fig. 8c), although not as efficiently as Trp.[105] The antioxidant melatonin (MLT) quenched azidyl radicals and formed MLT radicals in a similar way to Trp.[105] In contrast, other amino acids, including Tyr (tyrosine) and His, were unable to quench azidyl radicals despite of their important roles in electron transfer.[104,105]

A combined attack on peptides by photoactivated **13**, involving sequence-dependent platination and radical mechanisms, was observed using UHR-FT-ICR MS and EPR.[106] Two model peptides with amidated C-termini, Substance P (SubP) and [Lys]^3-Bombesin (K^3-Bom), were treated with **13** and irradiation. SubP gave rise to only mono-platinated adducts with different amino acids, while K^3-Bom showed both mono- and di-platinated adducts with a preference for His. In contrast, oxidation of SubP occurred only at Met, whereas oxidation of both Met and Trp was observed for K^3-Bom. Thioredoxin (Trx) is an important enzyme in the redox signalling pathway and is usually overexpressed in tumour cells.[107] Platination of His, Glu (glutamic acid), and Gln (glutamine) residues of Trx and oxidation of Met, Trp, and the Cys catalytic sites induced by **13** upon irradiation can inhibit the activity of Trx enzyme and Trx system, and further increase the cellular ROS level.[108]

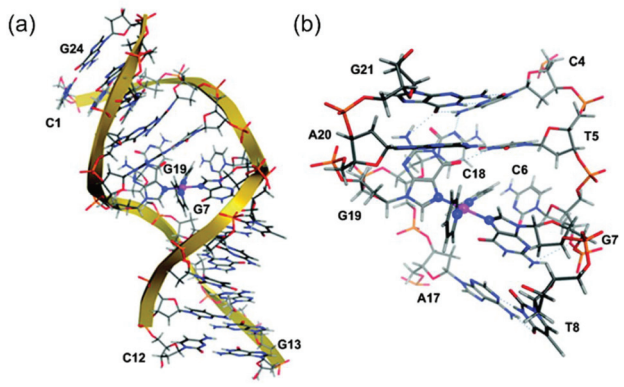

Fig. 7 (a) The average ligand field molecular dynamics (LFMD) structure of *trans*-$\{Pt(Py)_2\}^{2+}$-DNA derived from simulations; (b) an expanded view of the platinum-binding site showing the G_7–G_{19} interstrand cross-link within the DNA duplex dodecamer, d(5′-$C_1C_2T_3C_4T_5C_6G_7T_8C_9T_{10}C_{11}C_{12}$-3′)·d(5′-$G_{13}G_{14}A_{15}G_{16}A_{17}C_{18}G_{19}A_{20}G_{21}A_{22}G_{23}G_{24}$-3′). Adapted from ref. 103.

4.3. Effects on cancer cellular components and pathways

Photoreactions between photoactivated diazido Pt(IV) complexes and important biomolecules can result in the dysfunction of cellular components, changes to cellular morphology and disruption of cellular pathways, and eventually cell death.

The ability to damage DNA in intact cells has been investigated for both *cis* **2** and *trans* **3** using comet assays.[70] Both complexes produced DNA cross-links in living cells upon

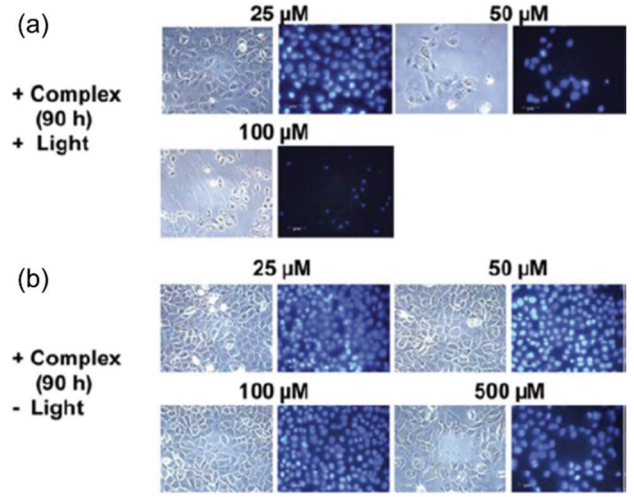

Fig. 9 Fluorescence microscopy images of 5637 cells treated by **2** with and without irradiation. Adapted from ref. 69.

irradiation and the effects were similar to those produced by cisplatin. When 5637 bladder cells were treated with **2** in the presence of light, dramatic changes in the morphology of the cells occurred, including cellular shrinkage, loss of adhesion with neighbouring cells, a large amount of nuclear packing, and nuclei disintegration, suggesting a different mechanism of cell death compared to cisplatin (Fig. 9).[69] None of these effects was observed without irradiation. Intriguingly, typical hallmarks of apoptosis, budding and cellular fragmentation, were not observed.

Single-cell electrophoresis experiments indicated that different DNA damage in HaCaT keratinocyte cells was caused by **6** and light with limited inhibition of DNA migration compared to cisplatin.[77] Also, p53 protein did not accumulate in cells, and caspase 3 activity was not detected when treated with **6** and irradiation, which was different from cells treated with cisplatin.[77] An autophagic mechanism was envisaged for **6** based on a significant increase in LC3B-II level and a decreased p62 level in treated cells.[78] Cell swelling and very little blebbing was seen for HL60 cells treated with irradiated **6**.[78] Notably, light activation was found to enhance the cellular accumulation of **6**.[79]

Excellent nuclear DNA binding properties were observed for photoactivated **13** that was shown to be a potent inhibitor to stall RNA pol II for RNA synthesis.[102] In contrast to cisplatin, photoactivated **13** did not produce fragmented or condensed nuclei, indicating a different mechanism.[81]

5. Derivatisation of photoactive diazido Pt(IV) complexes

The axial ligands (with arbitrary choice of OH as axial ligands) of photoactive Pt(IV) complexes can not only be released, similar to azide ligands, upon photoreduction to Pt(II), but also greatly affect the reduction potential of Pt(IV).[66,75] Generally, Pt(IV) complexes with a lower reduction potential (depending on the axial ligand: $I^- > Cl^- > OAc^- > OH^-$) exhibit higher stability to reductants.[60,66] Thus, the hydroxide ligands can enhance aqueous solubility and also stabilise the Pt(IV) oxidation state.[109] Modification of axial ligands is a feasible method to improve the selectivity and cytotoxicity of diazido-Pt(IV) complexes.

5.1. Multi-action diazido-Pt(IV) complexes

By combining photoactive Pt(IV) complexes with other anticancer active agents, such as stable radicals, enzyme inhibitors, and photosensitisers, multi-action prodrugs are obtained. Upon irradiation, these prodrugs release not only the reactive Pt(II) species and azidyl radicals, but also additional cytotoxic agents, enhancing the anticancer efficacy of the drugs. Owing to their different cellular targets and mechanism of action, combination of these cytotoxic species often results in a synergistic effect, producing greater cytotoxicity than that expected by simple addition of the two agents. Examples of diazido-Pt(IV) multi-action agents are summarised below.

Dinuclear complexes such as **16**, in which two molecules of **13** are bridged in an axial position by bisamide dicarboxylato linkers (Fig. 10) display similar photocytotoxicity towards cisplatin-resistant ovarian A2780cis and A2780 cells, and interestingly are relatively non-toxic toward normal cells (MRC-5 lung fibroblasts).[82]

The TEMPO radical has been conjugated to **13** since nitroxide radicals themselves can possess potent anticancer activity (**17**, Fig. 10).[110] The presence of the TEMPO radical in the complex was confirmed by EPR spectroscopy. Upon irradiation with blue light (420 nm), azidyl and TEMPO radicals were released, accompanied by the formation of toxic Pt(II) species.

Suberoyl-bis-hydroxamic acid (SubH) is a histone deacetylase (HDAC) inhibitor, which exhibits a profound dose-dependent inhibition of cancer cell proliferation.[111] Two SubH ligands have been attached to the axial positions of *cis*, *trans*-$[Pt(N_3)_2(OH)_2(t\mathrm{Bu}_2\mathrm{bpy})]$ to generate a diazido-Pt(IV) complex, *cis*, *trans*-$[Pt(N_3)_2(\mathrm{Sub})_2(t\mathrm{Bu}_2\mathrm{bpy})]$ (**18**, Fig. 10), that was stable

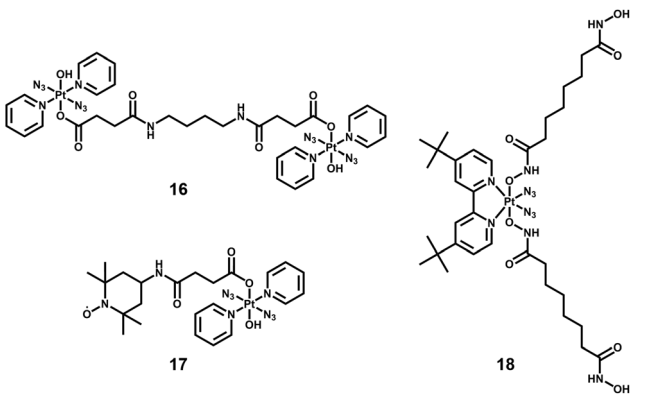

Fig. 10 Multi-action diazido-Pt(IV) complexes **16–18**.

in the dark.[112] Complex **18** released SubH and cytotoxic Pt(II) species, which targeted similar DNA regions as cisplatin efficiently upon UVA irradiation. Photoactivated **18** exhibited significant cytotoxicity in cancer cells with a low resistance factor compared with cisplatin and its Pt(IV) analogues containing inactive axial ligands. This suggested a different mechanism of action involving inhibition of HDAC that allowed platinum species to access chromatin DNA, introduced effective steric blockage of RNA polymerase II and formed DNA adducts (*e.g.* interstrand cross-links).

Metal complexes with curcumin ligands exhibit photo-induced anticancer activity.[113] Light activation of curcumin-loaded Dex-**2** nanoparticles **19** led to instant production of ROS by curcumin and released Pt(II) species from **2** (Fig. 11), and gave rise to photocytotoxicity and *in vivo* antitumour efficacy with low systemic toxicity to KM mice bearing subcutaneous H22 murine hepatocarcinoma tumour.[114]

The amphiphilic oligomer Ce6-PEG-Pt(IV) (CPP, **20**, Fig. 12) can self-assemble into micelles, and upconversion nanoparticles (UCNP) $NaYbF_4$: Tm@CaF_2 have been co-assembled to convert NIR into shorter wavelength irradiation that can induce decomposition of diazido-Pt(IV) complexes.[115] Micelles as self-assembled nanoparticles with a hydrophilic corona and hydrophobic core have been widely used in anticancer drug delivery.[116] Attachment of the photosensitiser Chlorin e6 to complex **2** resulted in an O_2-self generating PACT-PDT agent, where the photosensitiser relied on the oxygen produced by photoactivation of the diazido-Pt(IV) fragment to supply the oxygen required for PDT in hypoxic tissues. Dramatically enhanced photocytotoxicity was observed for this PACT-PDT system in hypoxic tumour models.

The nanoparticle-based agent **21** has complex **13** loaded onto silica-coated UCNP to allow photoactivation with NIR, together with a fluorescent probe that can be selectively switched-on in apoptotic conditions (Fig. 13a).[117] The probe included a fluorescence resonance energy transfer (FRET) pair, consisting of a far-red fluorescence donor Cy5 and a NIR quencher Qsy21, linked by a peptide sequence that can be recognised and cleaved by caspase-3, a key enzyme in apoptosis. Accordingly, when **21** was photoactivated by NIR irradiation, a chain reaction in A2780 ovarian cancer cells started on triggering apoptosis, thus activating caspase-3, which in turn cleaved the peptide-linker, switching on emission of the Cy5 dye and enabling imaging of apoptosis in living cells. Notably, when both peptide probe and Pt(IV) complex **13** were conjugated to human serum albumin protein (HSA, **22**, Fig. 13b), instead of UCNP, improved photocytotoxicity and real-time imaging was also achieved upon UVA irradiation.[118]

The nano-system **23**, combining Yb/Tm-codoped UCNP and **6**, exhibited better tumour inhibition under NIR irradiation than that under UV irradiation (Fig. 14).[119] Notably, this nano-system functioned as a theragnostic agent, whose therapeutic action could be informed and guided by different imaging modalities, such as upconversion luminescence (UCL), magnetic resonance (MR) and computer tomography (CT).

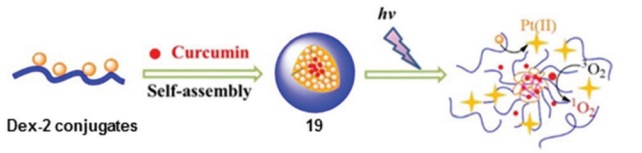

Fig. 11 Preparation and photodecomposition of curcumin-loaded Dex-**2** nanoparticles **19**. Adapted from ref. 114.

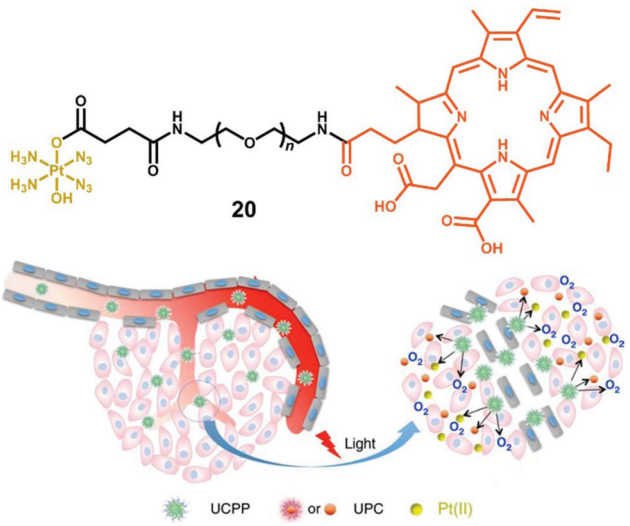

Fig. 12 The amphiphilic oligomer **20** and the photodecomposition of UCPP in a tumour microenvironment. Adapted from ref. 115.

5.2. Targeted delivery of diazido-Pt(IV) complexes

One of the major advantages of phototherapy over traditional chemotherapy is the ability to provide spatial and temporal control of the activation of prodrugs and their resulting cytotoxic activity. However, inefficient accumulation of photoactive prodrugs at the tumour site is still an issue and results in the

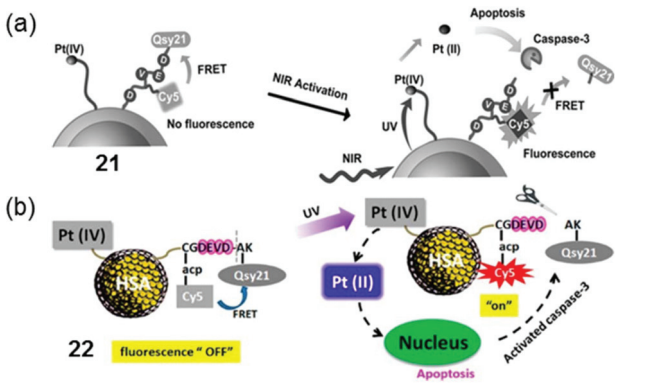

Fig. 13 Photoactivation of conjugates **21** and **22** based on (a) UNCP[117] and (b) HSA,[118] respectively. Adapted from ref. 117 and 118.

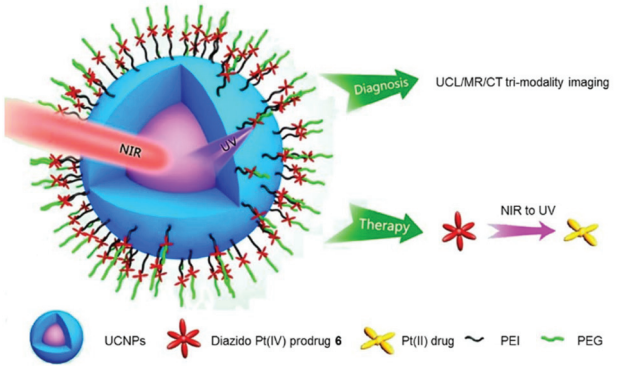

Fig. 14 Schematic illustration of the photodecomposition of conjugate **23**. Adapted from ref. 119.

need for higher concentrations to achieve therapeutic efficacy, increasing the risk of side effects. The conjugation of diazido Pt(IV) complexes with cancer-targeting vectors can improve their selectivity, increase their accumulation in cancer cells, and enable the prodrugs to be activated specifically within cancer cells.

Overexpression of particular receptors on the surface of cancer cells provides an excellent strategy for the targeted delivery of diazido-Pt(IV) complexes by tethering them to ligands that can bind selectively to those receptors. The RGD sequence (–Arg–Gly–Asp–) can be selectively recognised by $\alpha_v\beta_3$ and $\alpha_v\beta_5$ integrins that are overexpressed on the surface of several tumour cells and related to tumour angiogenesis.[120,121] The conjugate of photoactive Pt(IV) prodrug **13** and a cyclic RGD-containing peptide c(RGDfK) (**24**, Fig. 15) showed remarkably enhanced selectivity and increased cellular accumulation for cells overexpressing $\alpha_v\beta_3$ and $\alpha_v\beta_5$ integrins, although the IC_{50} values for irradiated cells were higher than those of its parent succinylated complex.[122] Another example of targeting for complex **13** is its conjugate with guanidinoneomycin, which is a RNA-binding ligand and allows the complex to be taken up by cancer cells in a selective proteoglycan-dependent manner (**25**, Fig. 15).[123] The photoproducts of Pt–guanidinoneomycin conjugate **25** with 5′-GMP or 5′-dCATGGCT were similar to that of the parent complexes under the same conditions. Similar to the Pt–c(RGDfK) conjugate, the Pt–guanidinoneomycin conjugate exhibited an enhanced cellular uptake with a preference for the SK-MEL-28 malignant melanoma cell line due to the expression of negatively charged cell-surface proteoglycans.

Nanoparticle-based drug delivery systems have attracted particular attention due to their enhanced accumulation in tumour tissue through the enhanced permeation and retention (EPR) effect caused by the leaky nature of angiogenic blood vessels in solid tumours.[88,124,125] The Pt^{IV}-N_3-FA@CDs nanoplatform **26** (Fig. 15) consisted of carbon dots decorated with the photoactive diazido Pt(IV) prodrug *cis*, *trans*, *cis*-$[Pt(N_3)_2(OH)_2(NH_3)(3\text{-}NH_2\text{-}Py)]$ and folic acid (FA) molecules, and exhibited a preference for folate receptor FR-positive

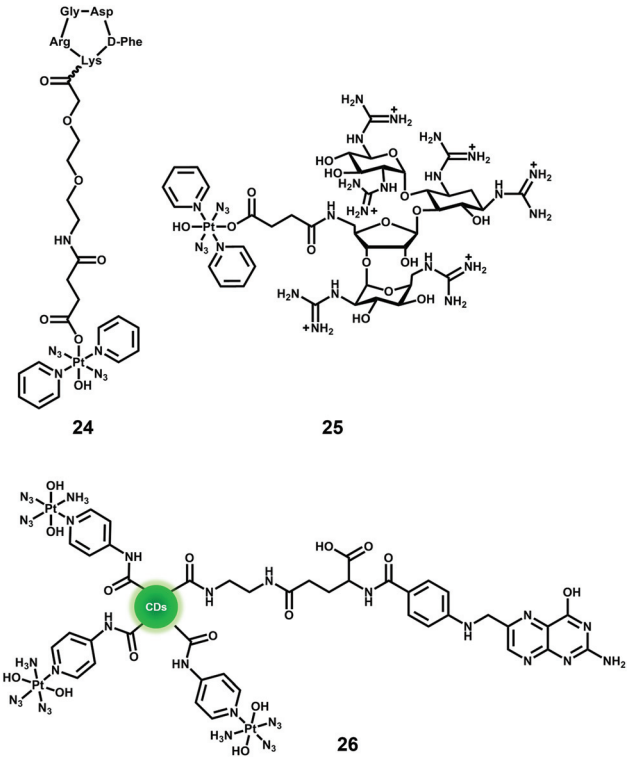

Fig. 15 Diazido-Pt(IV) complexes **24–26** with cancer cell-targeting vectors. CDs = carbon dots.

[FR(+)] human cervical HeLa cells over FR-negative [FR(–)] MCF-7 human breast tumour cells.[126]

Photo-responsive block copolymer (BCP) micelles have been widely investigated for their drug delivery applications in cancer therapy.[127] The triblock copolymer methoxy-poly (ethylene glycol)-*block*-poly(ε-caprolactone)-*block*-poly-L-lysine, $mPEG_{114}$-*b*-PCL_{20}-*b*-PLL_{10} that included mPEG (n = 114), poly-caprolactone (p = 20) and poly-L-lysine (q = 10) self-assembles in aqueous solution, with polycaprolactone and poly-L-lysine forming the core with Pt(IV) complex *cis*, *trans*-$[Pt(1R,2R\text{-}DACH)(N_3)_2(OH)_2]$ (DACH = 1,2-cyclohexanediamine) covalently encapsulated inside the hydrophobic core *via* an amide linkage (**27**, Fig. 16).[128] The micelles exhibit greatly enhanced cellular accumulation and photocytotoxicity to

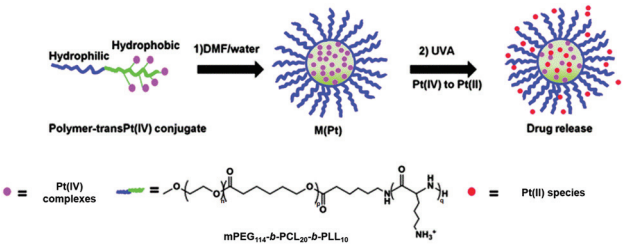

Fig. 16 The preparation and photodecomposition of micelles **27**,[128] **28**,[129] **29**[130] assembled by $mPEG_{114}$-*b*-PCL_{20}-*b*-PLL_{10} polymer with diazido Pt(IV) complexes. Adapted from ref. 129.

SKOV-3 ovarian cancer cells compared with polymer-free prodrugs. Importantly, *in vivo* studies revealed that conjugation to micelles enhanced the blood circulation half-life of the Pt(IV) complex by 10-fold and displayed improved inhibition efficacy against H22 murine hepatocarcinoma with decreased systemic toxicity. Complex **3** was also attached to the biodegradable polymer $mPEG_{114}$-*b*-PCL_{20}-*b*-PLL_{10} that can self-assemble into micelles with the hydrophobic chain and Pt species as the core to protect Pt(IV) prodrugs from potential deactivation in blood circulation.[129] The micelles **28** (Fig. 16) displayed comparable IC_{50} values to cisplatin upon irradiation and a resistance factor (IC_{50} ratio: A2780CDDP/A2780) 5× lower than cisplatin. When the same micelles incorporated sterically hindered **6**, they were proved to be >100 times more effective than cisplatin upon UVA irradiation (**29**, Fig. 16).[130]

The photocleavable tri-block copolymers PEG-PUPt(N_3)-PEG (PUPt(N_3) is polyurethane with repeating **13** bricks) produced a photosensitive micelle **30** (Fig. 17).[131] The *in vivo* experiments revealed that the irradiated micelle (430 nm) was 3–4× more effective to BALB/c nude mice bearing A549 xenografts than the prodrug and cisplatin with lowest body weight loss on day 27, suggesting lower systemic toxicity.

Complex **2**-loaded amphiphiles with one lactose motif self-assembled into micelles **31**, while the amphiphiles with two lactose motifs formed vesicles **32** instead (Fig. 18). These nanoparticles displayed photocytotoxicity with liver cancer-targeting ability *in vivo*. The platinum distribution in mice was determined by fluorescence, CT and ICP-MS.[132]

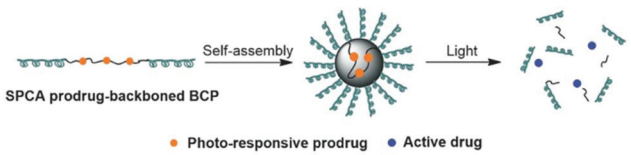

Fig. 17 The preparation and photodecomposition of micelles **30** assembled by a tri-block copolymer with complex **13**. Adapted from ref. 131.

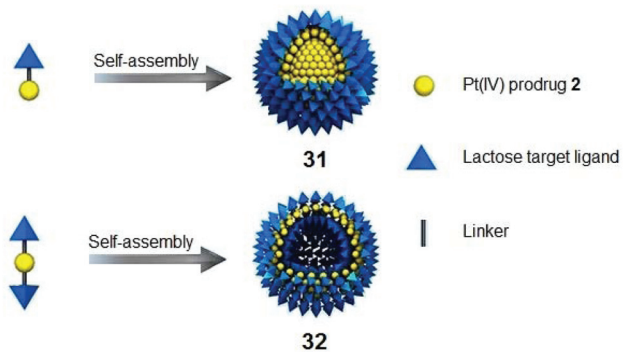

Fig. 18 Cancer-targeting micelles **31** and vesicles **32**. Adapted from ref. 132.

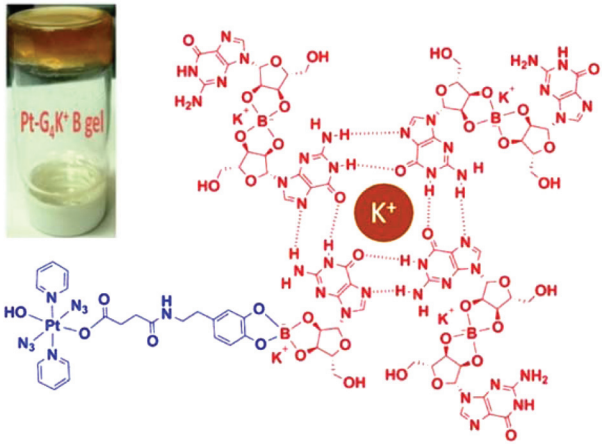

Fig. 19 Schematic illustration of self-assembled Pt-G_4K^+B anticancer hydrogel **33**. Adapted from ref. 136.

For surface tumours, such as non-melanoma skin cancer, topical medication is an ideal way for precise localisation. G_4K^+ hydrogels are biocompatible polymers with flexibility and high water content that allow them to mimic natural tissues.[133–135] Pt(IV)-based Pt-G_4K^+ B hydrogel **33** (Fig. 19) exhibited potent photocytotoxicity towards cisplatin-resistant A2780cis ovarian cancer cells while it displayed negligible cytotoxicity to MRC-5 normal fibroblast cells.[136]

6. Conclusions and prospects for clinical platinum photochemotherapy

Photoactive diazido-Pt(IV) complexes represent a new generation of platinum anticancer prodrugs that allow spatial and temporal control over their cytotoxic activity. They exhibit high dark stability, promising oxygen-independent photocytotoxicity, and novel mechanisms of action that allow them to circumvent cisplatin resistance. Modification of the prototype complexes (**1–15**), especially the axial ligands, improves their targeting ability and pharmacological properties. In this review, we have described the development of photoactive diazido-Pt(IV) complexes, including their cancer-targeting derivatives, and discussed their photodecomposition pathways, photoreaction with biomolecules, and their effect on cellular components and pathways.

Three main features of an ideal diazido-Pt(IV) complex for PACT appear to be crucial and need to be considered in any further development of these agents. (1) In contrast to cisplatin, *trans* geometry is more favourable than *cis* for diazido-Pt(IV) complexes, owing to the more intense and red-shifted LMCT bands, faster photodecomposition rate and improved photocytotoxicity. (2) The replacement of NH_3 by a π-acceptor pyridine ligand can not only red-shift the LMCT bands, but also enhance the cytotoxicity and introduce new mechanisms of action. Also, replacement of NH_3 by an aliphatic amine (*e.g.* CH_3NH_2) improves photocytotoxicity. (3) Axial derivatisation of

hydroxide/carboxylate ligands with cancer-targeting vectors or cytotoxic motifs provides an avenue for the design of new diazido-Pt(IV) complexes with improved selectivity, cellular accumulation and photocytotoxicity, longer activation wavelength, and convenient formulation.

In spite of the notable progress with research development of photoactive diazido-Pt(IV) complexes achieved so far, none of them has yet entered clinical trials. The achievement of longer wavelength activation for deeper tissue penetration, higher photocytoxicity indices, and tumour specific drug delivery remain major challenges to be further addressed. However, there are good prospects for use of such complexes for surface cancers such as bladder and oesophageal cancer. Hence there are encouraging signs that diazido-Pt(IV) complexes can provide novel PACT anticancer drugs with new mechanisms of action which can be effective against resistant cancers, so warranting further investigation.

Conflicts of interest

There are no conflicts to declare.

Acknowledgements

This research was supported by the MRC (grant G0701062), EPSRC (grants EP/G006792, EP/F034210/1, EP/P030572/1 to PJS), ERC (grant 247450 to PJS), a Chancellor's International PhD Scholarship from the University of Warwick (for HS), and the Wellcome Trust (209173/Z/17/Z, Sir Henry Wellcome Fellowship for CI).

Notes and references

1 R. L. Siegel, K. D. Miller and A. Jemal, *Ca-Cancer J. Clin.*, 2019, **69**, 7–34.
2 D. E. J. G. J. Dolmans, D. Fukumura and R. K. Jain, *Nat. Rev. Cancer*, 2003, **3**, 380–387.
3 N. J. Farrer, L. Salassa and P. J. Sadler, *Dalton Trans.*, 2009, **48**, 10690–10701.
4 S. Bonnet, *Dalton Trans.*, 2018, **47**, 10330–10343.
5 B. Rosenberg, L. Van Camp and T. Krigas, *Nature*, 1965, **205**, 698–699.
6 B. Rosenberg, L. Van Camp, J. E. Trosko and V. H. Mansour, *Nature*, 1969, **222**, 385–386.
7 L. Kelland, *Nat. Rev. Cancer*, 2007, **7**, 573–584.
8 S. C. Sweetman, *Martindale: The complete drug reference*, Pharmaceutical Press, London, 35th edn, 2007.
9 D. Wang and S. J. Lippard, *Nat. Rev. Drug Discovery*, 2005, **4**, 307–320.
10 B. W. Harper, A. M. Krause-Heuer, M. P. Grant, M. Manohar, K. B. Garbutcheon-Singh and J. R. Aldrich-Wright, *Chem. – Eur. J.*, 2010, **16**, 7064–7077.
11 T. C. Johnstone, K. Suntharalingam and S. J. Lippard, *Chem. Rev.*, 2016, **116**, 3436–3486.
12 L. Cai, C. Yu, L. Ba, Q. Liu, Y. Qian, B. Yang and C. Gao, *Appl. Organomet. Chem.*, 2018, **32**, e4228.
13 I. Kostova, *Recent Pat. Anti-Cancer Drug Discovery*, 2006, **1**, 1–22.
14 D. Gibson, *J. Inorg. Biochem.*, 2019, **191**, 77–84.
15 K. Mitra, *Dalton Trans.*, 2016, **45**, 19157–19171.
16 M. Coluccia, A. Nassi, F. Loseto, A. Boccarelli, M. A. Mariggio, D. Giordano, F. P. Intini, P. Caputo and G. Natile, *J. Med. Chem.*, 1993, **36**, 510–512.
17 K. S. Lovejoy, R. C. Todd, S. Zhang, M. S. McCormick, J. A. D'Aquino, J. T. Reardon, A. Sancar, K. M. Giacomini and S. J. Lippard, *Proc. Natl. Acad. Sci. U. S. A.*, 2008, **105**, 8902–8907.
18 P. Perego, C. Caserini, L. Gatti, N. Carenini, S. Romanelli, R. Supino, D. Colangelo, I. Viano, R. Leone, S. Spinelli, G. Pezzoni, C. Manzotti, N. Farrell and F. Zunino, *Mol. Pharmacol.*, 1999, **55**, 528–534.
19 A. M. Krause-Heuer, R. Grünert, S. Kühne, M. Buczkowska, N. J. Wheate, D. D. Le Pevelen, L. R. Boag, D. M. Fisher, J. Kasparkova, J. Malina, P. J. Bednarski, V. Brabec and J. R. Aldrich-Wright, *J. Med. Chem.*, 2009, **52**, 5474–5484.
20 T. Zou, C. Lok, Y. M. E. Funga and C. M. Che, *Chem. Commun.*, 2013, **49**, 5423–5425.
21 A. Naik, R. Rubbiani, G. Gasser and B. Spingler, *Angew. Chem., Int. Ed.*, 2014, **53**, 6938–6941.
22 J. P. Macquet and J. L. Butour, *J. Natl. Cancer Inst.*, 1983, **70**, 899–905.
23 X. Han, J. Sun, Y. Wang and Z. He, *Med. Res. Rev.*, 2015, **35**, 1268–1299.
24 J. L. Van der Veer, A. R. Peters and J. Reedijk, *J. Inorg. Biochem.*, 1986, **26**, 137–142.
25 R. M. Roat and J. Reedijk, *J. Inorg. Biochem.*, 1993, **52**, 263–274.
26 K. Lemma, J. Berglund, N. Farrell and L. I. Elding, *JBIC, J. Biol. Inorg. Chem.*, 2000, **5**, 300–306.
27 N. J. Wheate, S. Walker, G. E. Craig and R. Oun, *Dalton Trans.*, 2010, **39**, 8113–8127.
28 Q. Mi, S. S. Shu, C. X. Yang, C. Gao, X. Zhang, X. Luo, C. H. Bao, X. Zhang and J. Niu, *Clin. Eng. Radiat. Oncol.*, 2018, **7**, 231–247.
29 M. Gordon and S. Hollander, *J. Med.*, 1993, **24**, 209–265.
30 V. H. C. Bramwell, D. Crowther, S. O'Malley, R. Swindell, R. Johnson, E. H. Cooper, N. Thatcher and A. Howell, *Cancer Treat. Rep.*, 1985, **69**, 409–416.
31 M. J. McKeage, F. Raynaud, J. Ward, C. Berry, D. O'Dell, L. R. Kelland, B. Murrer, P. Santabárabara, K. R. Harrap and I. R. Judson, *J. Clin. Oncol.*, 1997, **15**, 2691–2700.
32 U. Olszewski, F. Ach, E. Ulsperger, G. Baumgartner, R. Zeillinger, P. Bednarski and G. Hamilton, *Met.-Based Drugs*, 2009, **2009**, 348916.
33 R. E. Cameron and A. B. Bocarsly, *Inorg. Chem.*, 1986, **25**, 2910–2913.
34 P. J. Bednarski, F. S. Mackay and P. J. Sadler, *Anticancer Agents Med. Chem.*, 2007, **7**, 75–93.

35 M. Imran, W. Ayub, I. S. Butler and Z. Rehman, *Coord. Chem. Rev.*, 2018, **376**, 405–429.
36 J. Šima, *Coord. Chem. Rev.*, 2006, **250**, 2325–2334.
37 V. Vreeken, M. A. Siegler, B. de Bruin, J. N. H. Reek, M. Lutz and J. I. Vlugt, *Angew. Chem., Int. Ed.*, 2015, **54**, 7055–7059.
38 A. Vogler and A. Kern, *Angew. Chem., Int. Ed. Engl.*, 1978, **17**, 524–525.
39 A. Vogler and J. Hlavatsch, *Angew. Chem., Int. Ed. Engl.*, 1983, **22**, 154–155.
40 A. Vogler, C. Quett and H. Kunkely, *Ber. Bunsen-Ges. Phys. Chem.*, 1988, **92**, 1486–1492.
41 P. J. Bednarski, K. Korpis, A. F. Westendorf, S. Perfahl and R. Grünert, *Philos. Trans. R. Soc., A*, 2013, **371**, 20120118.
42 X. Wang, X. Wang, S. Jin, N. Muhammad and Z. Guo, *Chem. Rev.*, 2019, **119**, 1138–1192.
43 N. J. Farrer and P. J. Sadler, *Aust. J. Chem.*, 2008, **61**, 669–674.
44 N. A. Smith and P. J. Sadler, *Philos. Trans. R. Soc., A*, 2013, **371**, 20120519.
45 P. Heringiova, J. Woods, F. M. Mackay, J. Kasparkova, P. J. Sadler and V. Brabec, *J. Med. Chem.*, 2006, **49**, 7792–7798.
46 Y. Zhao, G. M. Roberts, S. E. Greenough, N. J. Farrer, M. J. Paterson, W. H. Powell, V. G. Stavros and P. J. Sadler, *Angew. Chem., Int. Ed.*, 2012, **51**, 11263–11266.
47 K. Mitra, S. Gautam, P. Kondaiah and A. R. Chakravarty, *Angew. Chem., Int. Ed.*, 2015, **54**, 13989–13993.
48 K. Mitra, C. E. Lyons and M. C. T. Hartman, *Angew. Chem., Int. Ed.*, 2018, **57**, 10263–10267.
49 H. Shi, G. J. Clarkson and P. J. Sadler, *Inorg. Chim. Acta*, 2019, **489**, 230–235.
50 D. Liu, J. Ma, W. Zhou, W. He and Z. Guo, *Inorg. Chim. Acta*, 2012, **393**, 198–203.
51 K. L. Ciesienski, L. M. Hyman, D. T. Yang, K. L. Haas, M. G. Dickens, R. J. Holbrook and K. J. Franz, *Eur. J. Inorg. Chem.*, 2010, **15**, 2224–2228.
52 A. Presa, G. Vázquez, L. A. Barrios, O. Roubeau, L. Korrodi-Gregório, R. Pérez-Tomás and P. Gamez, *Inorg. Chem.*, 2018, **57**, 4009–4022.
53 A. Presa, R. F. Brissos, A. B. Caballero, I. Borilovic, L. Korrodi-Gregório, R. Pérez-Tomás, O. Roubeau and P. Gamez, *Angew. Chem., Int. Ed.*, 2015, **54**, 4561–4565.
54 S. Monro, K. L. Colón, H. Yin, J. Roque, P. Konda, S. Gujar, R. P. Thummel, L. Lilge, C. G. Cameron and S. A. McFarland, *Chem. Rev.*, 2019, **119**, 797–828.
55 Q. Chen, Z. Huang, D. Luck, J. Beckers, P. Brun, B. C. Wilson, A. Scherz, Y. Salomon and F. W. Hetzel, *Photochem. Photobiol.*, 2002, **76**, 438–445.
56 A. N. Hidayatullah, E. Wachter, D. K. Heidary, S. Parkin and E. C. Glazer, *Inorg. Chem.*, 2014, **53**, 10030–10032.
57 L. N. Lameijer, D. Ernst, S. L. Hopkins, M. S. Meijer, S. H. C. Askes, S. E. Le Dévédec and S. Bonnet, *Angew. Chem., Int. Ed.*, 2017, **56**, 11549–11553.
58 S. L. H. Higgins and K. J. Brewer, *Angew. Chem., Int. Ed.*, 2012, **51**, 11420–11422.
59 M. H. Al-Afyouni, T. N. Rohrabaugh, J. K. F. Al-Afyouni and C. Turro, *Chem. Sci.*, 2018, **9**, 6711–6720.
60 L. T. Ellis, H. M. Er and T. W. Hambley, *Aust. J. Chem.*, 1995, **48**, 793–806.
61 A. M. Pizarro, R. J. McQuitty, F. S. Mackay, Y. Zhao, J. A. Woods and P. J. Sadler, *ChemMedChem*, 2014, **9**, 1169–1175.
62 N. A. Kratochwil, P. J. Bednarski, H. Mrozek, A. Vogler and J. K. Nagle, *Anticancer Drug Des.*, 1996, **11**, 155–171.
63 N. A. Kratochwil, M. Zabel, K. J. Range and P. J. Bednarski, *J. Med. Chem.*, 1996, **39**, 2499–2507.
64 N. A. Kratochwil, J. A. Parkinson, P. J. Bednarski and P. J. Sadler, *Angew. Chem., Int. Ed.*, 1999, **38**, 1460–1463.
65 N. A. Kratochwil, Z. Guo, P. S. Murdoch, J. A. Parkinson, P. J. Bednarski and P. J. Sadler, *J. Am. Chem. Soc.*, 1998, **120**, 8253–8254.
66 N. A. Kratochwil and P. J. Bednarski, *Arch. Pharm. Pharm. Med. Chem.*, 1999, **332**, 279–285.
67 J. A. Duffy, *J. Phys. C: Solid State Phys.*, 1980, **13**, 2979–2989.
68 P. Müller, B. Schröder, J. A. Parkinson, N. A. Kratochwil, R. A. Coxall, A. Parkin, S. Parsons and P. J. Sadler, *Angew. Chem., Int. Ed.*, 2003, **42**, 335–339.
69 P. J. Bednarski, R. Grünert, M. Zielzki, A. Wellner, F. S. Mackay and P. J. Sadler, *Chem. Biol.*, 2006, **13**, 61–67.
70 F. S. Mackay, J. A. Woods, H. Moseley, J. Ferguson, A. Dawson, S. Parsons and P. J. Sadler, *Chem. – Eur. J.*, 2006, **12**, 3155–3161.
71 M. J. Cleare and J. D. Hoeschele, *Platinum Met. Rev.*, 1973, **17**, 2–13.
72 M. J. Cleare and J. D. Hoeschele, *Bioinorg. Chem.*, 1973, **2**, 187–210.
73 B. Rosenberg, L. Van Camp, E. B. Grimley and A. J. Thomson, *J. Biol. Chem.*, 1967, **242**, 1347–1352.
74 N. J. Farrer, J. A. Woods, V. P. Munk, F. S. Mackay and P. J. Sadler, *Chem. Res. Toxicol.*, 2010, **23**, 413–421.
75 H. C. Tai, Y. Zhao, N. J. Farrer, A. E. Anastasi, G. Clarkson, P. J. Sadler and R. J. Deeth, *Chem. – Eur. J.*, 2012, **18**, 10630–10642.
76 F. S. Mackay, S. A. Moggach, A. Collins, S. Parsons and P. J. Sadler, *Inorg. Chim. Acta*, 2009, **362**, 811–819.
77 F. S. Mackay, J. A. Woods, P. Heringová, J. Kašpárková, A. M. Pizarro, S. A. Moggach, S. Parsons, V. Brabec and P. J. Sadler, *Proc. Natl. Acad. Sci. U. S. A.*, 2007, **104**, 20743–20748.
78 A. F. Westendorf, J. A. Woods, K. Korpis, N. J. Farrer, L. Salassa, K. Robinson, V. Appleyard, K. Murray, R. Grünert, A. M. Thompson, P. J. Sadler and P. J. Bednarski, *Mol. Cancer Ther.*, 2012, **11**, 1894–1904.
79 A. F. Westendorf, L. Zerzankova, L. Salassa, P. J. Sadler, V. Brabec and P. J. Bednarski, *J. Inorg. Biochem.*, 2011, **105**, 652–662.
80 Y. Zhao, J. A. Woods, N. J. Farrer, K. S. Robinson, J. Pracharova, J. Kasparkova, O. Novakova, H. Li,

L. Salassa, A. M. Pizarro, G. J. Clarkson, L. Song, V. Brabec and P. J. Sadler, *Chem. – Eur. J.*, 2013, **19**, 9578–9591.
81 N. J. Farrer, J. A. Woods, L. Salassa, Y. Zhao, K. S. Robinson, G. Clarkson, F. S. Mackay and P. J. Sadler, *Angew. Chem., Int. Ed.*, 2010, **49**, 8905–8908.
82 H. Shi, I. Romero-Canelón, M. Hreusova, O. Novakova, V. Venkatesh, A. Habtemariam, G. J. Clarkson, J. Song, V. Brabec and P. J. Sadler, *Inorg. Chem.*, 2018, **57**, 14409–14420.
83 F. S. Mackay, N. J. Farrer, L. Salassa, H. C. Tai, R. J. Deeth, S. A. Moggach, P. A. Wood, S. Parsons and P. J. Sadler, *Dalton Trans.*, 2009, 2315–2325.
84 Y. Nakabayashi, A. Erxleben, U. Létinois, G. Pratviel, B. Meunier, L. Holland and B. Lippert, *Chem. – Eur. J.*, 2007, **13**, 3980–3988.
85 C. Loup, A. T. Vallina, Y. Coppel, U. Létinois, Y. Nakabayashi, B. Meunier, B. Lippert and G. Pratviel, *Chem. – Eur. J.*, 2010, **16**, 11420–11431.
86 L. Cubo, A. M. Pizarro, A. Gómez Quiroga, L. Salassa, C. Navarro-Ranninger and P. J. Sadler, *J. Inorg. Biochem.*, 2010, **104**, 909–918.
87 H. Xiao, L. Yan, E. M. Dempsey, W. Song, R. Qi, W. Li, Y. Huang, X. Jing, D. Zhou, J. Ding and X. Chen, *Prog. Polym. Sci.*, 2018, **87**, 70–106.
88 D. Guo, S. Xu, Y. Huang, H. Jiang, W. Yasen, N. Wang, Y. Su, J. Qian, J. Li, C. Zhang and X. Zhu, *Biomaterials*, 2018, **177**, 67–77.
89 A. Y. Sokolov and H. F. Schaefer III, *Dalton Trans.*, 2011, **40**, 7571–7582.
90 L. Ronconi and P. J. Sadler, *Chem. Commun.*, 2008, **2**, 235–237.
91 H. I. A. Phillips, L. Ronconi and P. J. Sadler, *Chem. – Eur. J.*, 2009, **15**, 1588–1596.
92 L. Salassa, H. I. A. Phillips and P. J. Sadler, *Phys. Chem. Chem. Phys.*, 2009, **11**, 10311–10316.
93 L. Ronconi and P. J. Sadler, *Dalton Trans.*, 2011, **40**, 262–268.
94 A. A. Shushakov, I. P. Pozdnyakov, V. P. Grivin, V. F. Plyusnin, D. B. Vasilchenko, A. V. Zadesenets, A. A. Melnikov, S. V. Chekalind and E. M. Glebov, *Dalton Trans.*, 2017, **46**, 9440–9450.
95 A. F. Westendorf, A. Bodtke and P. J. Bednarski, *Dalton Trans.*, 2011, **40**, 5342–5351.
96 A. F. Westendorf, *Synthese und Charakterisierung von photoaktivierbaren trans-Pt(IV)-Diaziden und Evaluierung iher DNA-bindenden und antiproliferativerenden Eigenschaften an Krebszellen unter Einfluss von Licht*, Dissertation, University of Greifswald, Germany, 2012.
97 Y. Zhao, N. J. Farrer, H. Li, J. S. Butler, R. J. McQuitty, A. Habtemariam, F. Wang and P. J. Sadler, *Angew. Chem., Int. Ed.*, 2013, **52**, 13633–13637.
98 R. R. Vernooij, T. Joshi, M. D. Horbury, B. Graham, E. I. Izgorodina, V. G. Stavros, P. J. Sadler, L. Spiccia and B. R. Wood, *Chem. – Eur. J.*, 2018, **24**, 5790–5803.
99 D. P. Bancroft, C. A. Lepre and S. J. Lippard, *J. Am. Chem. Soc.*, 1990, **112**, 6860–6871.
100 M. Crul, R. C. van Waardenburg, J. H. Beijnen and J. H. Schellens, *Cancer Treat. Rev.*, 2002, **28**, 291–303.
101 J. Kašpárková, F. S. Mackay, V. Brabec and P. J. Sadler, *JBIC, J. Biol. Inorg. Chem.*, 2003, **8**, 741–745.
102 J. Pracharova, L. Zerzankova, J. Stepankova, O. Novakova, N. J. Farrer, P. J. Sadler, V. Brabec and J. Kasparkova, *Chem. Res. Toxicol.*, 2012, **25**, 1099–1111.
103 H. C. Tai, R. Brodbeck, J. Kasparkova, N. J. Farrer, V. Brabec, P. J. Sadler and R. J. Deeth, *Inorg. Chem.*, 2012, **51**, 6830–6841.
104 J. S. Butler, J. A. Woods, N. J. Farrer, M. E. Newton and P. J. Sadler, *J. Am. Chem. Soc.*, 2012, **134**, 16508–16511.
105 C. Vallotto, E. Shaili, H. Shi, J. S. Butler, C. J. Wedge, M. E. Newton and P. J. Sadler, *Chem. Commun.*, 2018, **54**, 13845–13848.
106 C. A. Wootton, C. Sanchez-Cano, A. F. Lopez-Clavijo, E. Shaili, M. P. Barrow, P. J. Sadler and P. B. O'Connor, *Chem. Sci.*, 2018, **9**, 2733–2739.
107 A. Holmgren and J. Lu, *Biochem. Biophys. Res. Commun.*, 2010, **396**, 120–124.
108 J. Du, Y. Wei, Y. Zhao, F. Xu, Y. Wang, W. Zheng, Q. Luo, M. Wang and F. Wang, *Inorg. Chem.*, 2018, **57**, 5575–5584.
109 M. D. Hall and T. W. Hambley, *Coord. Chem. Rev.*, 2002, **232**, 49–267.
110 V. Venkatesh, C. J. Wedge, I. Romero-Canelón, A. Habtemariama and P. J. Sadler, *Dalton Trans.*, 2016, **45**, 13034–13037.
111 L. Ning, D. Y. Greenblatt, M. Kunnimalaiyaan and H. Chen, *Oncologist*, 2008, **13**, 98–104.
112 J. Kasparkova, H. Kostrhunova, O. Novakova, R. Křikavová, J. Vančo, Z. Trávníček and V. Brabec, *Angew. Chem., Int. Ed.*, 2015, **54**, 14478–14482.
113 S. Banerjee and A. R. Chakravarty, *Acc. Chem. Res.*, 2015, **48**, 2075–2083.
114 S. He, Y. Qi, G. Kuang, D. Zhou, J. Li, Z. Xie, X. Chen, X. Jing and Y. Huang, *Biomacromolecules*, 2016, **17**, 2120–2127.
115 S. Xu, X. Zhu, C. Zhang, W. Huang, Y. Zhou and D. Yan, *Nat. Commun.*, 2018, **9**, 2053.
116 S. S. Kesharwania, S. Kaurb, H. Tummala and A. T. Sangamwar, *Colloids Surf., B*, 2019, **173**, 581–590.
117 Y. Min, J. Li, F. Liu, E. K. L. Yeow and B. Xing, *Angew. Chem., Int. Ed.*, 2014, **53**, 1012–1016.
118 X. Li, J. Mu, F. Liu, E. W. P. Tan, B. Khezri, R. D. Webster, E. K. L. Yeow and B. Xing, *Bioconjugate Chem.*, 2015, **26**, 955–961.
119 Y. Dai, H. Xiao, J. Liu, Q. Yuan, P. Ma, D. Yang, C. Li, Z. Cheng, Z. Hou, P. Yang and J. Lin, *J. Am. Chem. Soc.*, 2013, **135**, 18920–18929.
120 M. Friedlander, P. C. Brooks, R. W. Shaffer, C. M. Kincaid, J. A. Varner and D. A. Cheresh, *Science*, 1995, **270**, 1500–1502.
121 J. S. Desgrosellier and D. A. Cheresh, *Nat. Rev. Cancer*, 2010, **10**, 9–22.
122 A. Gandioso, E. Shaili, A. Massaguer, G. Artigas, A. González-Cantó, J. A. Woods, P. J. Sadler and V. Marchán, *Chem. Commun.*, 2015, **51**, 9169–9172.

123 E. Shaili, M. Fernández-Giménez, S. Rodríguez-Astor, A. Gandioso, L. Sandín, C. García-Vélez, A. Massaguer, G. J. Clarkson, J. A. Woods, P. J. Sadler and V. Marchán, *Chem. – Eur. J.*, 2015, **21**, 18474–18486.
124 H. Maeda, *J. Controlled Release*, 2012, **164**, 138–144.
125 H. Wei, R. Zhuo and X. Zhang, *Prog. Polym. Sci.*, 2013, **38**, 503–535.
126 X. Yang, H. Xiang, L. An, S. Yang and J. Liu, *New J. Chem.*, 2015, **39**, 800–804.
127 Y. Zhao, *Macromolecules*, 2012, **45**, 3647–3657.
128 H. Xiao, G. T. Noble, J. F. Stefanick, R. Qi, T. Kiziltepe, X. Jing and B. Bilgicer, *J. Controlled Release*, 2014, **173**, 11–17.
129 H. Song, W. Li, R. Qi, L. Yan, X. Jing, M. Zheng and H. Xiao, *Chem. Commun.*, 2015, **51**, 11493–11495.
130 H. Song, X. Kang, J. Sun, X. Jing, Z. Wang, L. Yan, R. Qi and M. Zheng, *Chem. Commun.*, 2016, **52**, 2281–2283.
131 D. Zhou, J. Guo, G. B. Kim, J. Li, X. Chen, J. Yang and Y. Huang, *Adv. Healthcare Mater.*, 2016, **5**, 2493–2499.
132 S. He, C. Li, Q. Zhang, J. Ding, X. Liang, X. Chen, H. Xiao, X. Chen, D. Zhou and Y. Huang, *ACS Nano*, 2018, **12**, 7272–7281.
133 G. M. Peters, L. P. Skala, T. N. Plank, B. J. Hyman, G. N. M. Reddy, A. Marsh, S. P. Brown and J. T. Davis, *J. Am. Chem. Soc.*, 2014, **136**, 12596–12599.
134 G. M. Peters, L. P. Skala, T. N. Plank, H. Oh, G. N. M. Reddy, A. Marsh, S. P. Brown, S. R. Raghavan and J. T. Davis, *J. Am. Chem. Soc.*, 2015, **137**, 5819–5827.
135 T. N. Plank and J. T. Davis, *Chem. Commun.*, 2016, **52**, 5037–5040.
136 V. Venkatesh, N. K. Mishra, I. Romero-Canelón, R. R. Vernooij, H. Shi, J. P. C. Coverdale, A. Habtemariam, S. Verma and P. J. Sadler, *J. Am. Chem. Soc.*, 2017, **139**, 5656–5565.